

# Local Solutions of the Optimal Power Flow Problem

W. A. Bukhsh,, A. Grothey, K. I. M. McKinnon, and P. A. Trodden

## Abstract

The existence of locally optimal solutions to the AC optimal power flow problem (OPF) has been a question of interest for decades. This paper presents examples of local optima on a variety of test networks including modified versions of common networks. We show that local optima can occur because the feasible region is disconnected and/or because of nonlinearities in the constraints. Standard local optimization techniques are shown to converge to these local optima. The voltage bounds of all the examples in this paper are between  $\pm 5\%$  and  $\pm 10\%$  off-nominal. The examples with local optima are available in an online archive [1] and can be used to test local or global optimization techniques for OPF. Finally we use our test examples to illustrate the behaviour of a recent semi-definite programming approach that aims to find the global solution of OPF.

## Index Terms

Optimal Power Flow; Local optima; global optimum.

## I. INTRODUCTION

Optimal power flow (OPF) is a well studied optimization problem in power systems. This problem was first introduced by Carpentier [2] in 1962. The objective of OPF is to find a steady state operating point that minimizes the cost of electric power generation while satisfying operating constraints and meeting demand. The problem can be formulated as a nonlinear programming (NLP) problem, in which some constraints and possibly the objective function are nonlinear. In the usual polar coordinate formulation of OPF the major nonlinearity in the constraints is in Kirchhoff's voltage laws (KVL), which gives the flow of power in a transmission line as a nonlinear function of bus voltages and phase angles. The presence of the nonlinear equality constraints results in the feasible region of the OPF problem being nonconvex [3] and hence raises the possibility of the existence of local OPF solutions. However in the 1997 paper [4] one of the authors states that in practice OPF solutions are unique, and this remains a common perception.

The first solution method for the OPF problem was proposed by Dommel and Tinney [5] in 1968, and since then numerous other methods have been proposed. A good literature survey of classical optimization techniques as applied to OPF over the last 30 years is given in [6], [7]. None of these methods are guaranteed to find the global minimum if a local one exists.

The issue of the possible existence of local optima to the OPF problem is an important one, but one that is not well covered in the literature. A recent literature survey [8] of OPF covers evolutionary algorithms

This work is supported by the UK Engineering and Physical Sciences Research Council (EPSRC) under grant EP/G060169/1.

Waqquas Bukhsh, Andreas Grothey and Ken McKinnon are with the School of Mathematics, University of Edinburgh, James Clerk Maxwell Building, Edinburgh EH9 3JZ, Scotland (e-mail: w.a.bukhsh@sms.ed.ac.uk, a.grothey@ed.ac.uk, k.mckinnon@ed.ac.uk)

P. A. Trodden is with the Department of Automatic Control & Systems Engineering, University of Sheffield, Mappin Street, Sheffield S1 3JD, UK (e-mail: p.trodden@shef.ac.uk).

as well as classical local nonlinear techniques. Evolutionary algorithms are global optimization techniques that attempt to find global optima. Global techniques are much slower than the local ones so should only be used for problems where local optima may exist. The authors of [9] discuss the role of metaheuristic techniques to solve the OPF problem and give the possible convergence to local solutions as a major drawback of classical optimization techniques applied to OPF. However, none of these surveys give any reference to examples of local optima of OPF or estimate how often these occur in practice.

The OPF problem has been extended in various ways. For example security constrained OPF and risk based OPF deal with the problem of ensuring the network operates securely. However if local optima exist for the original OPF problem they will in principle also exist for extensions, so in this paper we restrict attention to the standard OPF problem.

In [10] the authors give an interesting semi-definite program (SDP) formulation of a dual of the OPF problem. They show that if there is no duality gap a globally optimal solution to the OPF can be recovered from the SDP dual, and they give a condition, which can be tested after solving the SDP dual, that guarantees there is no duality gap. It is however not obvious just from the properties of a general network whether or not there will be a duality gap and it is not clear how often the method works in practice. Sufficient conditions for there to be no duality gap that rely only on network properties are given in [11] and [12]. These apply to tree networks and networks with lossless loops and require fixed voltage magnitudes, limits on the angle difference across lines and/or significant flexibility in the real and reactive power balance at buses. However these conditions are not met in general networks or in any of the examples in this paper. Some of the shortcomings of the SDP approach are discussed in [13]. In [14] examples are given of modified IEEE test cases where the SDP recovery strategy fails, and a branch and bound strategy using the SDP formulation for the relaxations is proposed that find the global optima in these cases. However none of these cases have documented local OPF solutions.

In order to support the current research interest in optimization techniques for OPF problem, it is important to have test cases with known local optima. It is well known that the power flow equations can have solutions with very low voltages at some buses. By relaxing the voltage bounds in standard test networks we have found corresponding low voltage local solutions for the OPF problem. These low voltage solutions however are not of practical interest and are excluded in OPF problems by reasonable voltage bounds. In this paper, we give examples of local solutions of OPF within reasonable voltage bounds: all examples either have  $\pm 5\%$  bounds or the same bounds as the standard cases from which they are derived (where the most extreme voltages are within  $\pm 10\%$ ). The modifications made to the standard test cases are either to reduce demand or change the generator power limits. All other system properties are unchanged. Some of the changes in generator power limits are significant, but in no cases are the optimal generator outputs unrealistic. The data for the test cases, their network diagrams and all the local solutions we have found are available in the online archive [1].

The layout of the paper is as follows. In Section II the OPF problem is introduced and its relation to the load flow problem is described. In Section III we show the existence of local OPF solutions for four specially constructed simple networks. Section IV investigates the occurrence of local solutions on

IEEE and other standard networks and shows that local solutions are not found but do occur after suitable changes to load levels or generator limits. In Section V the reasons for occurrence of local solutions are discussed. Section VI illustrates the behaviour of the SDP optimization method of [10] on 2- and 3-bus cases and reports its success or failure on the other test cases. Conclusions are given in Section VII.

## II. OPTIMAL POWER FLOW (OPF)

The OPF problem can be formulated using either polar or rectangular coordinates. In polar coordinates the variables are the voltage magnitude and phase angle at each bus and the real and reactive power flows. Any angle can be changed by a multiple of  $2\pi$  without changing the other variables, so these give equivalent solutions and are not counted as distinct local solutions. In the rectangular coordinates the bus voltages are represented by their real and imaginary components. Since the voltage magnitudes must be positive for a feasible solution the mapping between polar and rectangular coordinates is one to one and continuous in the neighbourhood of any feasible point. Consequently local solutions in polar coordinates give rise to local solution in rectangular coordinates and vice versa, so the number of local optima in rectangular coordinates is the same as the number of non-equivalent local solutions in polar coordinates. In this paper the polar formulation is used.

### A. OPF in polar coordinates

Consider a power system network with the set of generators  $\mathcal{G}$ . Let  $\mathcal{G}_b$  and  $\mathcal{D}_b$  be the set of generators and demands at bus  $b$ , let  $\mathcal{B}_b$  be the set of buses connected by a line to bus  $b$ , and let  $b_0$  be the reference (or slack) bus. Parameters  $v_b^{\text{LB}}$  and  $v_b^{\text{UB}}$  are the lower and upper bounds on variable  $v_b$ , the voltage at bus  $b$ ; parameters  $P_g^{\text{LB}}$  and  $P_g^{\text{UB}}$  are the bounds on variable  $p_g^G$ , the real power output of generator  $g$ ; parameters  $Q_g^{\text{LB}}$  and  $Q_g^{\text{UB}}$  are the bounds on variable  $q_g^G$ , the reactive power output of generator  $g$ ; and parameters  $P_d^D$  and  $Q_d^D$  are the real and reactive power consumed by load  $d$ , which are assumed to be independent of voltage. Variables  $p_{bb'}^L$  and  $q_{bb'}^L$  are the real and reactive power flowing into line  $bb'$  from bus  $b$ , and parameter  $S_{bb'}^{\text{max}}$  is the apparent power line rating of the line  $bb'$ . Variable  $\theta_b$  is the voltage phase angle at bus  $b$ .

The OPF problem is to minimize the cost of generation while supplying all the load and satisfying the bus voltage limits, the apparent power line limits and the real and reactive generator output power limits. It can be written as:

$$\min \sum_{g \in \mathcal{G}} f(p_g^G), \quad (1)$$

subject to

$$\sum_{g \in \mathcal{G}_b} p_g^G = \sum_{d \in \mathcal{D}_b} P_d^D + \sum_{b' \in \mathcal{B}_b} p_{bb'}^L + G_b^B v_b^2, \quad (2)$$

$$\sum_{g \in \mathcal{G}_b} q_g^G = \sum_{d \in \mathcal{D}_b} Q_d^D + \sum_{b' \in \mathcal{B}_b} q_{bb'}^L - B_b^B v_b^2, \quad (3)$$

$$\begin{aligned} p_{bb'}^L &= v_b^2 G_{bb} \\ &+ v_b v_{b'} (G_{bb'} \cos(\theta_b - \theta_{b'}) + B_{bb'} \sin(\theta_b - \theta_{b'})), \end{aligned} \quad (4)$$

$$\begin{aligned} q_{bb'}^L &= -v_b^2 B_{bb} \\ &+ v_b v_{b'} (G_{bb'} \sin(\theta_b - \theta_{b'}) - B_{bb'} \cos(\theta_b - \theta_{b'})), \end{aligned} \quad (5)$$

$$\theta_{b_0} = 0, \quad (6)$$

$$v_b^{\text{LB}} \leq v_b \leq v_b^{\text{UB}}, \quad (7)$$

$$P_g^{\text{LB}} \leq p_g \leq P_g^{\text{UB}}, \quad (8)$$

$$Q_g^{\text{LB}} \leq q_g \leq Q_g^{\text{UB}}, \quad (9)$$

$$p_{bb'}^{L^2} + q_{bb'}^{L^2} \leq (S_{bb'}^{\max})^2, \quad (10)$$

where (1) is the objective function, equations (2)–(3) are Kirchhoff's Current Law (KCL) enforcing real and reactive power balance, (4)–(5) are KVL, (6) removes the degeneracy in the bus voltage angles by fixing it to zero at the arbitrary reference bus, (7)–(9) are constraints on voltage and power generation, and (10) are the line flow constraints. The line conductance  $g_{bb'}$  and susceptance  $b_{bb'}$  are defined by

$$g_{bb'} = \frac{r_{bb'}}{r_{bb'}^2 + x_{bb'}^2}, \quad b_{bb'} = \frac{-x_{bb'}}{r_{bb'}^2 + x_{bb'}^2},$$

where  $r_{bb'}$ ,  $x_{bb'}$  are the line resistance and reactance, and parameters  $G_{bb'}$  and  $B_{bb'}$  are defined by

$$g_{bb'} = -\tau_{bb'} G_{bb'} = -\tau_{bb'} G_{b'b} = G_{b'b'} = \tau_{bb'}^2 G_{bb}, \quad (11)$$

$$b_{bb'} + 0.5b_{bb'}^C = B_{b'b'} = \tau_{bb'}^2 B_{bb}, \quad (12)$$

$$-b_{bb'} = \tau_{bb'} B_{b'b} = \tau_{bb'} B_{bb'}, \quad (13)$$

where  $b_{bb'}^C$  is the line charging susceptance and  $\tau_{bb'} = 1$  except in transformer “lines”, where it is the tap ratio and (as in the MATPOWER [15] convention) the ideal transformer is at the  $b$  end of the line. Also we assume none of the transformers have a phase shift, which is true for all examples in the paper.

The constraints (6)–(10) are convex, and in all the examples referred to in this paper the generator costs are convex (linear or quadratic). However (2)–(5) are nonlinear equality constraints and therefore nonconvex. Consequently the polar coordinate formulation is nonconvex and so local optima cannot be ruled out. With a slight redefinition of  $p_{bb'}^L$  and  $q_{bb'}^L$  it is possible to transfer the nonlinear terms in the KCL to the KVL equations leaving the KCL equations linear. It is also possible to eliminate equations

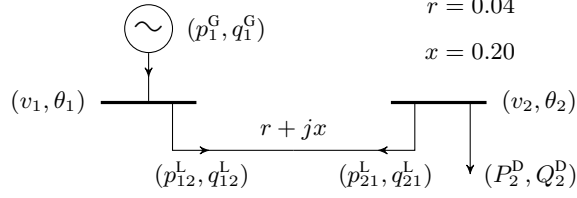


Fig. 1. WB2 2-bus system.

(4)–(5) and instead use them to eliminate  $p_{bb}^L$  and  $q_{bb}^L$  from (4)–(5) and (10). However neither of these reformulations change the solutions in terms of the bus voltages and angles and generator outputs, so they do not change the number of local optima present.

### B. OPF in rectangular coordinates

In the rectangular OPF formulation the bus voltages are represented by the real and imaginary voltage components [16], and the real and reactive power flows are quadratic functions of these. This results in the generator limits, the fixed loads and the apparent power line limits being nonconvex constraints, and in addition the lower limits of bus voltage magnitudes are nonconvex. Hence the rectangular formulation is also nonconvex, so once again local optima cannot be ruled out.

### C. Relation of OPF to load flow problems

If we fix all demands, and the voltages at all generator buses, and the generator outputs at all generator buses except one (referred to as the slack bus), and also fix the phase angle at the slack bus, then we can use equations (2)–(5) to solve for the remaining variables. This is the load flow problem [16] and it is well known that it can have 0, 1 or multiple solutions [17], [18]. Provided a load flow solution satisfies all the line limits and the bounds on voltages and generator outputs imposed in OPF it will be a feasible solution for OPF. We shall now present a simple load flow example with multiple solutions, and in the following section extend this to illustrate one reason for local solution of OPF existing.

Consider the 2-bus network shown in Fig. 1. Bus 2 is the load bus, and bus 1 is the generator bus and slack bus, and for it we set  $v_1 = 0.95$  and  $\theta_1 = 0$ . If we know the load at bus 2 then it is possible to find the remaining variables  $(p_g, q_g, v_2, \theta_2)$ . There are at most two possible load flow solutions. Fig. 2 shows these solutions when the load at Bus 2 is  $(P_2^D, Q_2^D) = t(350, -350)$  for  $t \geq 0$ . Note the load here is capacitative and so reactive power is *injected* from the load into bus 2. For a load corresponding to  $t < 1.004$  there are two alternative solutions. The solid branch corresponds to lower real power generation (the better case) and to higher voltage at bus 2, and the dotted branch corresponds to higher real power generation and lower voltage. Moreover, we can see that as the load increases the two solutions get closer and eventually coalesce at a point. Beyond this there are no solutions – *i.e.*, the line loading limit has been reached.

In this example the solutions come together at a voltage that is feasible, however if the load is changed from capacitative to inductive the voltage at the coalescing point drops to an infeasibly low value. The

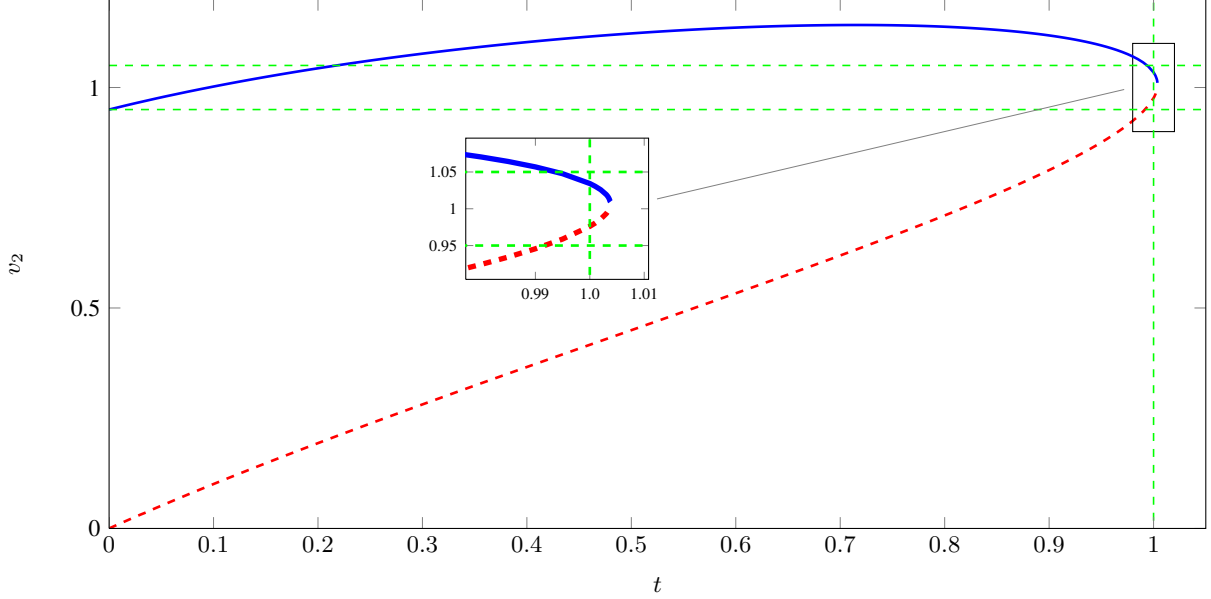


Fig. 2. Alternate load flow solutions as the demand parameter,  $t$ , varies.

solution space of a general 2-bus system is discussed in [19].

### III. CONSTRUCTED OPF NETWORKS WITH LOCAL OPTIMA

In this section we present examples, WB2, WB3 and WB5, of simple radial and meshed/loop networks we have constructed to illustrate local optima. These examples have no line limits and have voltage limits within  $\pm 5\%$  off-nominal, and WB2 and WB3 have no generator limits. However all the optimal solutions have reasonable generator outputs and line flows. We also document local optima in a contrasting example, LMBM3, which is the 3-bus example in [13] but with a different line limit.

#### A. Local solutions in 2-, 3- and 5-bus networks

Consider first a 2-bus OPF example, WB2, based on the network in Fig. 1 with  $t$  fixed at the value 1.0, which gives fixed real and reactive loads of 350.0 MW and  $-350.0$  Mvar respectively. This is close to the nose of the curve in Fig. 2. In Section II-C, the slack bus voltage was fixed at  $v_1 = 0.95$  to obtain Fig. 2. In OPF problems this voltage is one of the degrees of freedom, and in a one generator example it is the only degree of freedom. Now set the voltage limits on both buses to  $[0.95, 1.05]$ .

The feasible region is shown by the thick lines in Fig. 3. It consists of two disconnected sections. The objective is the real power generated,  $p^G$ , and the global minimum is at  $S_1$  on the solid (blue) curve, at which point  $v_1 = 0.952$ . Higher values of  $v_1$  would reduce the objective but would cause  $v_2$  to rise above 1.05, which is its upper limit. On the dotted (red) section of the feasible region the optimal point is  $S_2$ . This is a local optima as it is the best point in its neighbourhood. Both solutions are given in Tab. I.

This 2-bus example shows that OPF problems can have local solutions with reasonable voltages. However as with the load flow case this relies on there being a net injection of reactive power at the load. This could be due to a fixed capacitor, or a generator with positive lower bound on reactive power

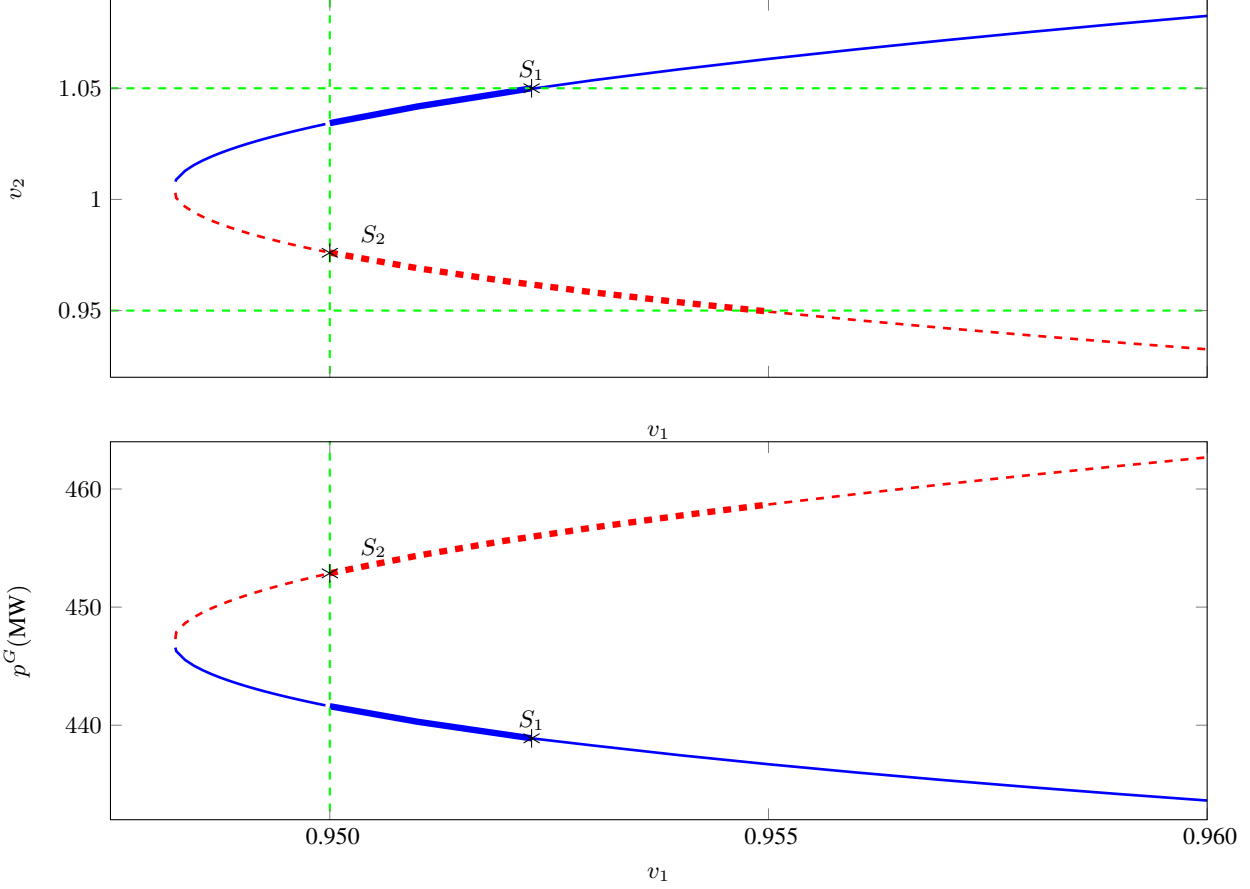


Fig. 3. WB2 2-bus system. Dependency of bus 2 voltage,  $v_2$ , and generator real power  $p^G$  on bus 1 voltage  $v_1$ . Feasible region shown by thick lines.

generation. A more common cause of excess reactive power is cables injecting reactive power when their flow is low. This motivates the next example.

A 3-bus network, WB3, in which bus 2 and bus 3 are connected via a cable is shown in Fig. 4. The cable is identical to one in the 24-bus IEEE test case. Loads are in MW and Mvar and neither is capacitative. Results are given in Tab. II:  $S_1$  is the global solution and  $S_2$  is the local solution.

In each of the above examples the objective values are proportional to the real power output of the single generator, and in both cases the local and global optimum are very close. This is because the difference in cost is due only to the different power losses in the lines and these losses are small compared to the

TABLE I  
OPF SOLUTIONS FOR THE WB2 2-BUS PROBLEM.

	Cost	Bus	$v$ (p.u.)	$\theta$ (deg)	$p^G$ (MW)	$q^G$ (Mvar)
$S_1$	877.78	1	0.952	0.00	438.89	94.44
		2	1.050	-57.14		
$S_2$	905.73	1	0.950	0.00	452.86	164.32
		2	0.976	-64.94		

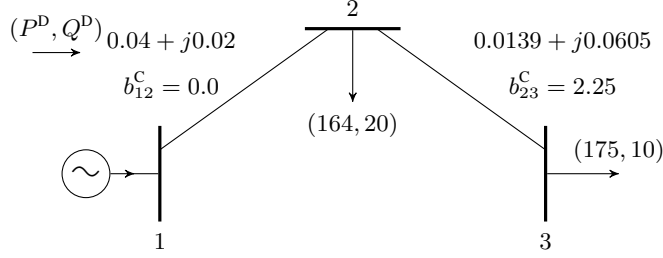


Fig. 4. WB3 3-bus system.

power transferred.

To get a bigger difference in the objective values there needs to be more than one generator with different costs. A 5-bus network, WB5, with two generators with different costs is given in the archive [1]. This system has two optimal solutions, the local being 14% more expensive than the global. The lower limits on the generators reactive power output are active at one generator in both solutions.

In the above examples, in all the standard test cases and in the cases derived from them in this paper except for the 39-bus case, the line limits are large and are inactive at all optimal solutions. Also in most cases with local optima there is an excess of reactive power in the network. In contrast, the 3-bus example LMBM3 in [13], shown in Fig. 5, has an apparent power limit  $S_{32}^{\max}$  on line 3–2 but no other line limits. There are no positive or negative limits on the reactive power outputs of the generators at buses 1 and 2 or the synchronous condenser at bus 3. The real power output of the generators can be any nonnegative value (and is 0 for the synchronous condenser). Voltage limits are  $\pm 10\%$  off-nominal. The cost of generator  $g$  is  $C^L p_g^G + C^Q (p_g^G)^2$ , independent of reactive power output. Since there is unlimited reactive power available at every bus, the reactive power constraints are redundant and the results are independent of the reactive loads. When  $S_{32}^{\max} = 186$  there are 5 optimal solutions; see Tab. III. If the voltage limits are tightened to  $\pm 5\%$  the perturbation of  $S_3$  becomes infeasible leaving 4 solutions.

### B. Local solutions in loop networks

In power transmission networks there is usually more than one path between pairs of buses, and such networks contain loops. It has been shown that for networks containing loops there can be multiple load

TABLE II  
OPF SOLUTIONS FOR WB3 3-BUS PROBLEM WITH CABLE.

	Cost	Bus	$v$ (p.u.)	$\theta$ (deg)	$p^G$ (MW)	$q^G$ (Mvar)
$S_1$	417.25	1	0.951	0.00	208.62	8.93
		2	0.950	-27.25		
		3	0.981	-30.36		
$S_2$	418.14	1	0.950	0.00	209.07	-20.79
		2	1.011	-26.36		
		3	1.050	-29.23		

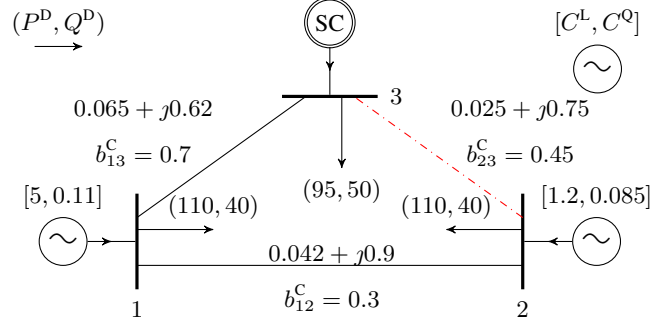


Fig. 5. LMBM3 3-bus system.

TABLE III  
OPF SOLUTIONS FOR LMBM3 3-BUS SYSTEM WITH  $S_{32}^{\max} = 186$ .

	Total Cost	Bus	$v$ (p.u.)	$\theta$ (deg)	$p^G$ (MW)
$S_1$	5694.54	1	1.100	0.00	128.46
		2	1.100	9.00	188.22
		3	1.100	-11.64	0.00
$S_2$	6833.94	1	0.900	0.00	124.78
		2	0.900	128.59	223.07
		3	0.900	-35.81	0.00
$S_3$	7684.42	1	1.033	0.00	186.45
		2	0.900	125.81	178.68
		3	0.900	-69.79	0.00
$S_4$	7966.67	1	0.900	0.00	181.17
		2	0.900	32.18	194.54
		3	0.900	-132.22	0.00
$S_5$	9677.11	1	0.900	0.00	231.75
		2	1.100	-108.01	168.32
		3	1.047	173.27	0.00

flow solutions corresponding to different integer multiple of  $2\pi$  for the phase shift round the loop [20], [21], and this phenomenon has been repeatedly observed to occur in real power systems [21]. We now present an example of this that gives rise to local OPF solutions.

The network shown in Fig. 6 consists of single loop with an even number  $n$  of buses. The loads are at the even buses and the generators at the odd. Every load is the same and every line has the same impedance. If all generators have identical real and identical reactive power outputs, then in the solution of the load flow the voltage magnitudes at all generator buses are equal and the voltage magnitudes at all load buses are equal. For each integer value of  $m$  there is a solution with voltage angle at bus  $k$  given by

$$\theta_k = \begin{cases} \frac{2\pi m}{n}(k-1) & k = 1, 3, \dots, n-1 \\ \frac{2\pi m}{n}(k-2) + \alpha & k = 2, 4, \dots, n \end{cases} \quad (14)$$

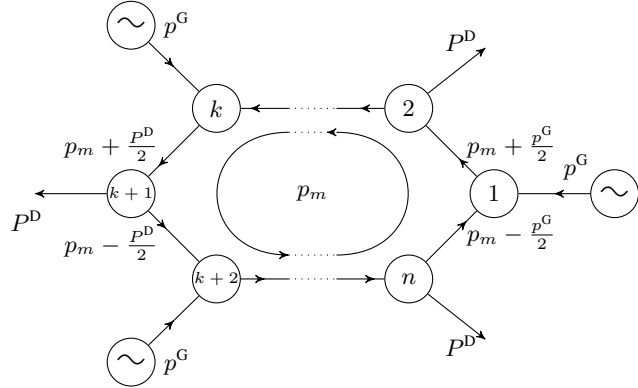


Fig. 6. Solutions in  $n$ -bus loop network (showing only real flows).

where  $\alpha$  is the voltage angle at bus 2. The corresponding real power flows are shown in Fig. 6. If  $m = 0$  then the circulating flow,  $p_m$ , is 0, the voltage angles at the generator buses are all 0 and the angles at the load buses are all  $\alpha$ . If  $m \neq 0$  then  $p_m$  is nonzero and there is a circulating flow.

In the corresponding OPF problem different generators can have different outputs. If all the generators have the same cost then it is optimal (verified computationally in Sec. IV) for all generators to have the same output. Hence the above flows are optimal. Fig. 6 with  $p_m = 0$  is the global solution. When  $p_m \neq 0$  there is a circulating flow which results in extra line losses, so this gives a local solution. For the network where  $n = 22$ ,  $z = 0.01 + j0.05$ ,  $(P^D, Q^D) = (204.25, 43)$ ,  $\pm 5\%$  voltage limits and all generators with the same cost, the  $m = 0$  case gives the global solution and  $m = \pm 1$  cases give the only local solutions, which are 31% more expensive. Tab. IV gives the solutions and Fig. 7 shows the complex voltages. If the voltage bounds are widened to  $\pm 10\%$  off-nominal the  $m = \pm 2$  case is also feasible and the local optima are 28% and 132% more expensive than the global solution.

#### IV. SEARCHING FOR LOCAL OPF SOLUTIONS

In this section we report the results of a computational search for local OPF solutions in standard test networks and in slightly modified versions of them, as well as in the cases described in Sec. III. The standard cases tested were the IEEE 14-, 24-, 30-, 57-, 118- and 300-bus cases as specified in the archive [22] and the 9 and 39 bus case from the MATPOWER test library [15]. In these examples most of the voltage limits are either 5% or 6% above or below nominal and all limits are within 10%. In our

TABLE IV  
TWO OPF SOLUTIONS FOR THE 22-BUS LOOP NETWORK.

	Bus	$v$ (p.u.)	$\alpha$ (deg)	$p^G$ (MW)	$q^G$ (Mvar)
$S_1$	$k$ odd	1.050		206.31	53.30
	$k$ even	1.029	-2.60		
$S_2$	$k$ odd	1.015		269.519	369.28
	$k$ even	0.950	13.33		

modifications of the standard cases the only change to the voltage limits is to tighten the limits in the 39 bus case from  $\pm 6\%$  to  $\pm 5\%$ .

It is important to be aware that an NLP solver may converge to a point that is not a local optimum, either by reaching (or by chance being started at) a stationary but non-optimal point or simply through an unreported solver error. For example MATPOWER with MIPS or fmincon-IPM falsely identifies a local optimum in the network in [23]. In order to avoid mistakenly classifying a point as a local optimum we check that the first order optimality conditions are satisfied and also that several NLP solvers converge to it when started from several random points in a small box surrounding it. The optimization systems used were MATPOWER [15] using fmincon with default settings, and the NLP solvers IPOPT [24], KNITRO [25] and SNOPT [26] each called from an AMPL model. For the problems in this paper we found no cases where any of these solvers converged to a solution that was non-optimal.

A second common mode of failure for any nonlinear solver is for it to converge to an infeasible point. This occurs in some of the cases reported later, however were such a case to occur in a real world OPF case then it would be identified and the search repeated from a different starting point. This is therefore not such a serious problem as finding a local optimum without realizing there is a better global solution.

To find local solutions we generated a random point within the bounds of each variable using a uniform distribution, and solved the OPF problem starting from this initial point. For each test case this process was repeated over 2000 times. There is however no guarantee even with such a large number of searches that all optima have been found.

When applied to the examples in Sec. III the method found all the reported solutions (and no others). When applied to the unmodified standard test cases no local solutions were found, and this was true also if the quadratic terms in the objective were omitted. However after scaling down the demand, modifying the generator bounds or tightening the voltage bounds the local optima described below were found. Full specifications of all the solutions are available at [1].

#### *A. 9-bus case*

When the reactive power generation lower bounds on all three generators were raised from  $-300$  Mvar to  $-5$  Mvar and all loads scaled to 60%, then 4 optimal solutions were found. The cost of the worst local solution is 37% more than the cost of global solution.

#### *B. 39-bus case*

When the loads were halved and the voltage limits tightened from  $\pm 6\%$  to  $\pm 5\%$ , two OPF solutions were found. The local solution cost was 115% above the global solution. When in addition only the linear cost coefficients were used, 16 solutions were found. These solutions have very different generation levels, however they are all within 0.5% in objective value. The reason for this is that the generators have identical cost functions so in the linear case, the difference in the objective values is due only to the different losses in the network.

### C. 118-bus case

When the generators' real and reactive power bounds were all relaxed by scaling them by a factor of 7, then three optimal solutions were found. The cost of the local solutions were 38% and 51% greater than the global solution.

### D. 300-bus case

The 300-bus case was modified as in the 9-bus case (*i.e.*, the lower limits on generator reactive power are changed to  $-5$  Mvar and load scaled down to 60%). This change in the generator bounds tightens some and relaxes others. Then 7 optimal OPF solutions were found, and the worst local solution had a cost 2.5% above the global solution.

### E. Starting point in local search

In all the above cases random starting points were used to find different local optima. If solving an OPF problem only once then it is more natural to start from a flat start: *i.e.*, the point with all voltage angles 0, all bus voltage magnitudes 1 and all generator injections at the mid point of the bounds. From a flat start IPOPT found the global optimum in all the cases in this paper, but MATPOWER with MIPS (the default solver) converged to a local optimum for WB5. To investigate further we took the modified 9-, 39-, 118- and 300-bus cases (which have local optima) and for each generated 200 cases by randomly perturbing their costs. This yielded 649 cases with local optima and for these cases we tested how often the global minimum was found starting from the flat start and from random points. This showed that the flat start was significantly better than random points: from a flat start IPOPT converged to a local but not global minima in 2.6% of cases and to an infeasible point in 0.3% of cases, compared to 23.2% and 1.4% respectively from the random points.

## V. REASONS FOR LOCAL OPTIMA

In this section we analyse reasons for the occurrence of the local optima reported in Sec. III and IV. All the examples of local optima in this paper have one or more of the following features: disconnected feasible region, loop flow, an excess of real or reactive power, or large voltage angles differences across lines. Each of these features is discussed below.

Local optima of optimization problems may lie within a connected part of the feasible region or be in different disconnected parts. When the feasible region is disconnected then the optima within each region must be a local optima for the whole problem, so there are at least as many optima as disconnected feasible regions.

A disconnected feasible region occurs because of the interaction of the nonlinear KCL and KVL equations with the remaining constraints (which are convex). It can be seen from Fig. 3 that the feasible space of the 2-bus case is disconnected, and that this is due to the interaction of the lower voltage limit on  $v_1$  with the other constraints. If this lower limit is relaxed to below 0.948, then the solid and dotted curves in Fig. 3 join within the feasible region. The feasible region is then connected and the local optimum disappears. A similar analysis shows this is also the reason for the local optima in the 3-bus example.

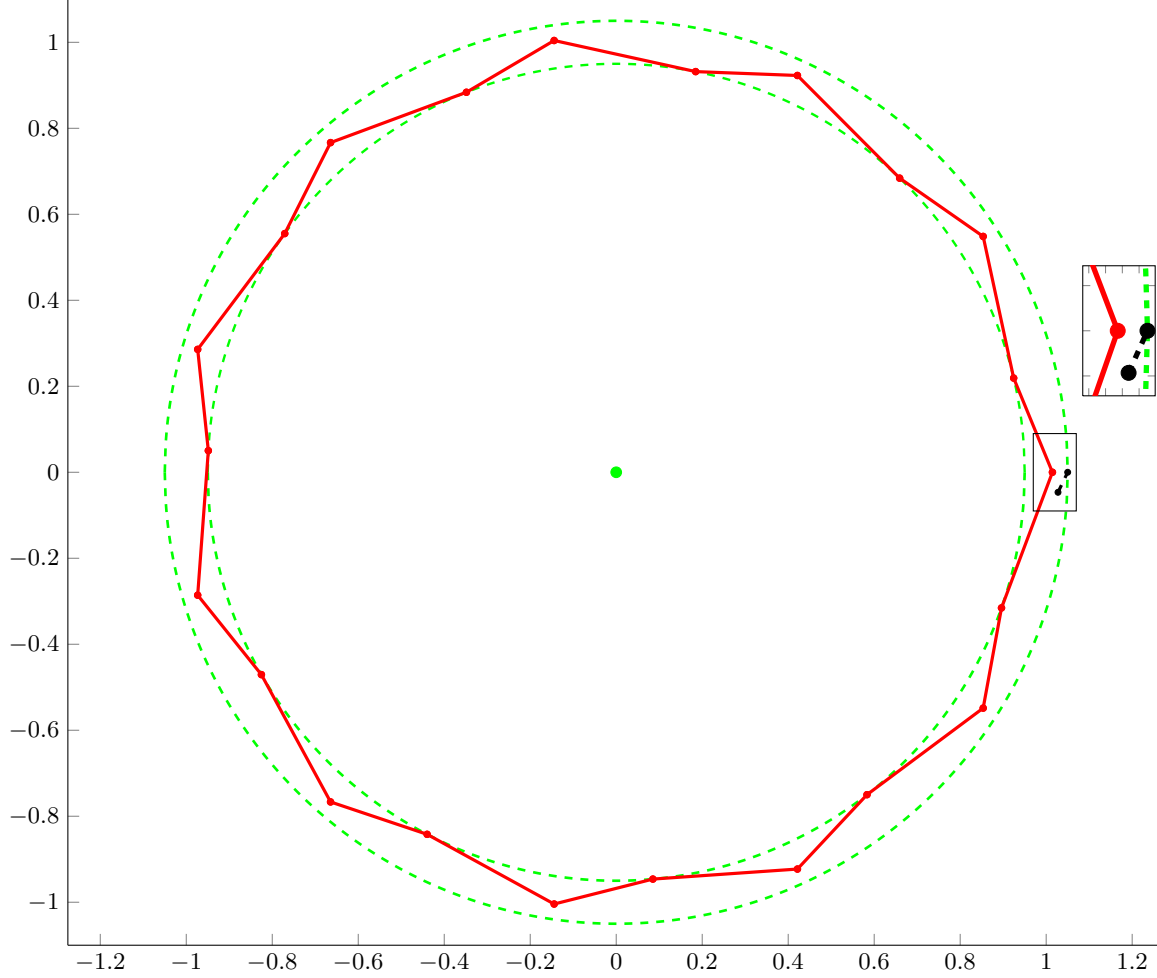


Fig. 7. Real and imaginary voltages (in p.u.) for the 2 solutions of the 22-bus loop case. The loop flow solution has red solid lines and the non loop flow has the black dashed line. The two circles show the  $\pm 5\%$  voltage limits.

Whenever there is a loop in a network there is the possibility of load flow solutions analogous to alternative solutions in the loop network example of Sec. III-B. Fig. 7 shows the complex bus voltages in rectangular coordinate for the loop (solid) and non-loop (dotted) solutions of the loop network of Fig. 6 with  $n = 22$  and with  $\pm 5\%$  off-nominal voltage limits. The edges correspond to lines in the network. In the non-loop optimal solution the voltages at generator buses are all the same and the voltages at the load buses are all the same, so there are only two distinct bus voltages on the plot and all the edges coincide. For the loop flow there is a closed connected path surrounding the origin whereas for the non-loop flow this is not the case. If the bus voltages are moved continuously from their values in the loop flow to their values in the non-loop flow (with the straight edges following) there must be a stage where the closed path moves from surrounding to origin to not surrounding it. At that stage the origin lies on one of the (straight) edges and so the angle across the corresponding line is  $\pi$ .

This is the point of maximum line loss and in most practical cases this will be excluded by a some constraint, for example on apparent power, that limits the phase angle difference across the line. When such constraints exists then the loop and non-loop flows are in disconnected parts of the feasible region

(and so local optima must exist). Even if there are no constraints that limit line angles, it is likely that other constraints on generation level or voltage will prevent line angles passing through  $\pi$ . This is the situation in the 22-bus loop network (which has loops with phase cycles of  $2\pi$  and  $4\pi$ ) and the 118-bus case (in which the more expensive local solution has loops with a  $2\pi$  phase cycle). As a result these are disconnected from the global optima. In LMBM3 the voltage plots of  $S_3$  and  $S_5$  surround the origin but the voltage plots of  $S_1$ ,  $S_2$  and  $S_4$  do not. The feasible region has two disconnected parts, with all except  $S_3$  in one of them. When  $S_5$  is moved continuously to  $S_1$ , then line 1–3 passes through  $\pi$ , but this is possible because line 1–3 has no limit. However the combination of the line limit on 3–2 and the bus voltage limits make it impossible to move continuously from  $S_3$  to a feasible solution with a line angle of  $\pi$  on either of the other lines, so the feasible region is disconnected.

In the other cases of local optima it is not obvious whether or not they lie in the same connected region. To check this we used the method described in the Appendix to try to find a continuous path connecting the local optima. If a path is found the local optima must lie in the same connected part of the feasible region. Paths were found between  $S_1$ ,  $S_2$ ,  $S_4$  and  $S_5$  in LMBM3 and between all the local optima in each of the 39- and 300-bus cases, so showing they lie in the same connected region. However in all other cases no path was found between the local optima. This is consistent with the previous analysis of WB2, WB3, LMBM3, and the 22-bus loop and 118-bus cases which we know have disconnected feasible regions. This leaves WB5 and the 9-bus case as the only uncertain cases.

In Sec. III we noted that in WB2 a local solution within reasonable voltage limits required the load to be capacitative (which injects reactive power), and in WB3 a cable was needed (which also generates reactive power). Also in WB5 the lower limits on generator reactive power output were active. No local solutions were found in the 9-, 39- and 300-bus networks with the default loads, but were found once the loads were reduced and/or the generator reactive power lower limits were increased. Since loads normally absorb reactive power, reducing loads leaves more reactive power in the network. Also lower loads lead to lower line flows and this results in less reactive power being absorbed by lines and eventually results in most lines becoming sources of reactive power. These two effects together can result in an excess of reactive power in the network and reactive power marginal prices that are negative.

When there is an excess of reactive power it would improve the solution if lines were able to absorb more reactive power. However in a line with phase angle  $\Delta\theta$  the reactive power absorbed and the real power lost are each proportional to  $1 - \cos(\Delta\theta)$ . It is therefore not possible by varying only voltage angles to increase the reactive power absorbed in a line without also increasing the real power lost. In situations where the reactive power excess is not high there is no advantage in increasing both the absorption and loss, however when the reactive power excess is high this can be an advantage. There is then an advantage in having a high value of  $1 - \cos(\Delta\theta)$ , which occurs with either small or large  $\Delta\theta$ , and this dichotomy is a potential cause of local optima.

A related though rarer situation is when there is an excess of real power in the network with corresponding negative real power marginal prices (making it worthwhile to pay consumers to increase their demand or suppliers to reduce their generation). This occurs for example in the local optima of WB2 and

WB3, and could occur in any network due to the loss of a large load. It is then again advantageous to increase  $1 - \cos(\Delta\theta)$ , in this case so as to lose real power in the lines. When negative generation costs are introduced to the standard test problems most of them then have many local optima. In [13] it is observed that the situation of negative real power marginal price is one in which the SDP method can fail.

Finally in some networks the generator and line limits are so wide that they allow very large voltage angles across lines and bus voltages that spread over a wide area of the voltage diagram. The feasible region is then significantly nonconvex and local optima can occur. This is the situation in LMBM3 and in the modified 118 bus case (in which the generator limits were relaxed). In every local optima for these cases some line angle is greater than  $145^\circ$ . In contrast the line angles for all the optima in WB2 are less than  $65^\circ$ , in WB5 are less than  $49^\circ$  and in all other cases are less than  $30^\circ$ .

## VI. PERFORMANCE OF SDP METHOD ON TEST CASES

The authors of [10] propose a semi-definite programming (SDP) relaxation of the OPF problem. They show that if a certain sufficient condition is satisfied, there is no duality gap between the original problem and the convex SDP dual, and that the globally optimal OPF solution can be recovered. The sufficient condition states that a certain matrix,  $A^{\text{opt}}$ , must have exactly two zero eigenvalues. The value of  $A^{\text{opt}}$  depends on the dual solution and it is not clear from the properties of the system alone whether or not the condition will hold, nor is it clear how often it holds in practice. We now investigate how well the method works on the examples in this paper.

Consider the family of problems for the 2-bus network of Fig. 1 obtained by varying  $v_2^{\text{UB}}$ , the upper bound on  $v_2$ , over the range  $[0.95, 1.06]$ . When  $v_2^{\text{UB}} \geq 1.035$  there are two solutions with the global one lying on the solid branch. (Tab. I and Fig. 3 show these solutions when  $v_2^{\text{UB}} = 1.05$ ). When  $v_2^{\text{UB}} < 1.035$  the  $S_1$  solution is excluded and the global optimum now lies on the dotted branch. As  $v_2^{\text{UB}}$  decreases from 0.976 the optimal solution moves from  $S_2$  to the right along the dotted curve. The optimal objective value is the primal curve in Fig. 8.

When the SDP dual method is applied to this problem with  $v_2^{\text{UB}} \geq 1.035$  it correctly identifies  $S_1$  as the global solution, and for  $v_2^{\text{UB}} \leq 0.976$  it correctly identifies the global solution lying on the dotted branch. In both of these ranges exactly two of the four eigenvalues of  $A^{\text{opt}}$  are nonzero (which is the sufficient condition for the SDP dual method to give the global solution). However when  $0.976 < v_2^{\text{UB}} < 1.035$  the SDP method returns an objective value which is an average of the values at  $v_2^{\text{UB}} = 0.976$  and  $v_2^{\text{UB}} = 1.035$ , all four eigenvalues are zero and the process of recovering a primal solution fails. The SDP dual objective value is the dotted curve in Fig. 8. The gap between the primal and dual curves is positive for the same range of  $v_2^{\text{UB}}$  values for which the SDP dual method fails to recover the optimal solution. The lower graph in Fig. 8 shows how the magnitude of the eigenvalues of  $A^{\text{opt}}$  depend on  $v_2^{\text{UB}}$ . Two of the eigenvalues are always zero and the other two are equal.

The number of local optima in LMBM3 depends on the value of  $S_{32}^{\text{max}}$ , the apparent power limit on line 3–2. The objective values of the 5 solutions over the ranges where they are feasible are shown in Fig. 9. The  $\times$  on the graphs show where (as it increases) the line limit becomes inactive. The maximum

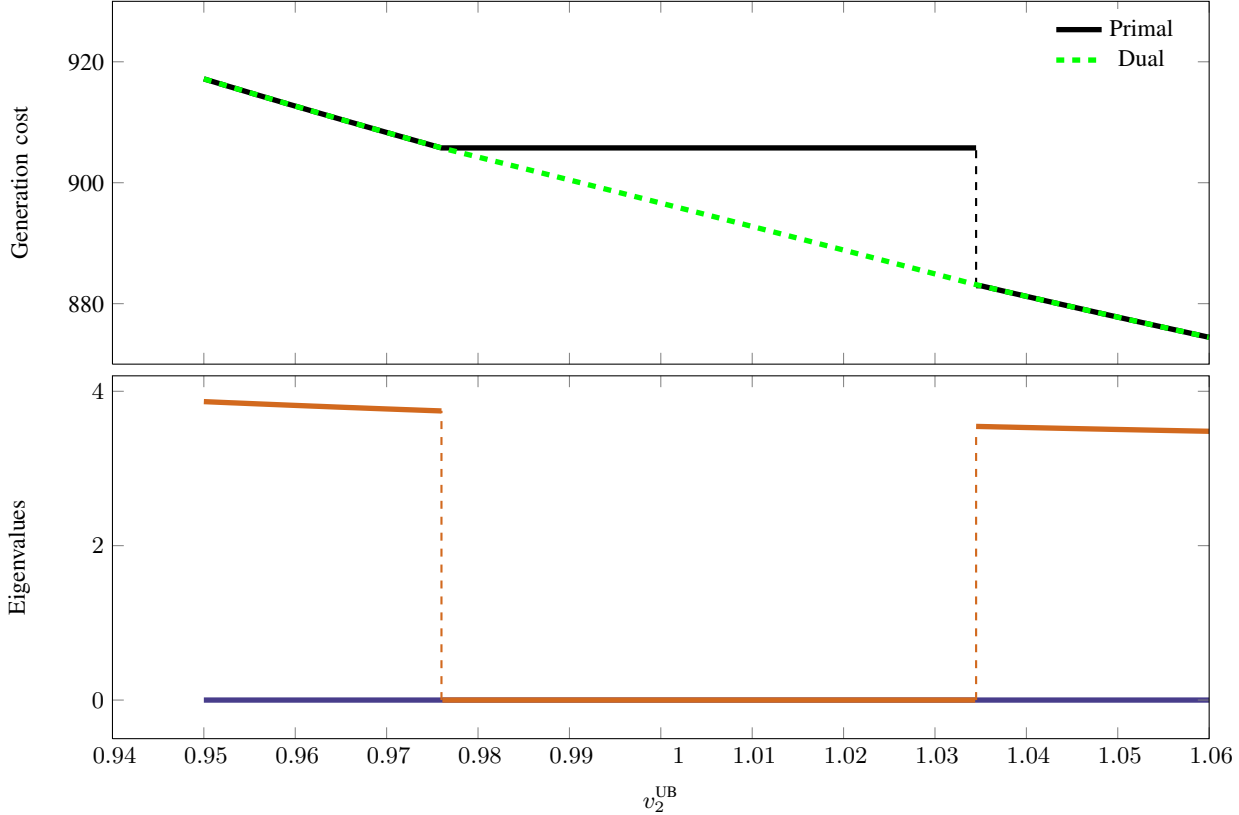


Fig. 8. Performance of SDP optimization method on 2-bus problem.

apparent power that can enter a line with the properties of line 3–2 occurs when the line angle is close to  $\pi$ . When the voltages are 0.9, the minimum, the corresponding apparent power is 187.55 Mvar, so when  $S_{32}^{\max}$  is larger than this it does not prevent the line angle passing through  $\pi$ . With this limit removed  $S_3$  and  $S_4$  stop being local optima so their graphs disappear. The minimum possible apparent power entering a line with the properties of line 3–2 is 28.33 Mvar and so if  $S_{32}^{\max}$  is below this there are no feasible solutions. The reason for the lower limit of the ranges of  $S_2$ ,  $S_3$  and  $S_5$  is that the curvature changes and the local optima disappears below the limit. Fig. 9 also shows the solution of the SDP dual. The method recovers the global solution for all value of  $S_{32}^{\max}$  above 52.7, and fails for all lower values. This is consistent with [13] where it was shown to fail when  $S_{32}^{\max} = 50$  and succeed when  $S_{32}^{\max} = 60$ .

In WB5 the lower bound on reactive power of generator 2,  $Q_2^{\text{LB}}$ , affects both the number of local solutions and the success of the SDP method. The SDP method succeeds for  $Q_2^{\text{LB}} < -30.8$  and fails otherwise. Local optima exist for  $-40 \leq Q^{\text{LB}}$ , so for  $-40 \leq Q_2^{\text{LB}} \leq -30.8$  local optima exist and the SDP method works.

The SDP method successfully found the global minimum in all the standard test cases except for the 39-bus case. However these problems do not have local optima. When applied to the problems with local optima the SDP approach worked successfully for WB3 and the 22-bus loop case with default bounds and for some parameter values for WB2, WB5 and LMBM3, but it failed in all other cases. As suggested in [10] we have added a positive resistance to all transformer lines which have zero resistance. (We tested

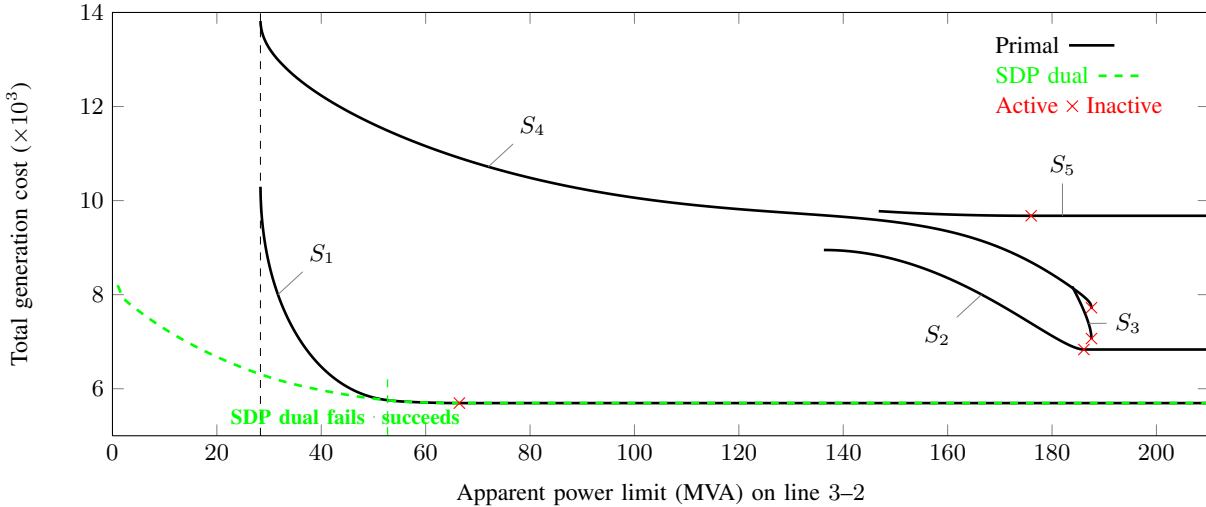


Fig. 9. Primal and dual objectives of the LMBM3 3-bus problem.

TABLE V  
NUMBER OF LOCAL SOLUTIONS AND OUTCOME OF SDP METHOD.

Case	$n^B$	# of solutions	SDP Method
WB2	2	2	Succeeds/Fails
WB3	3	2	Succeeds
WB5	5	2	Succeeds/Fails
LMBM3	3	5	Succeeds/Fails
case9mod	9	4	Fails
case22loop	22	2	Succeeds
case39mod1	39	2	Fails
case39mod2	39	16	Fails
case118mod	118	3	Fails
case300mod	300	7	Fails

values from  $10^{-5}$  to  $10^{-3}$  per unit.) Without this modification the sufficient condition for zero duality gap cannot hold, however in the above failure cases it is not enough to ensure the sufficient condition holds. Tab. V gives a summary of the results when applied to the problems with local optima.

## VII. CONCLUSION

In this paper, we have shown the existence of local solutions of OPF problems. All examples have either  $\pm 5\%$  voltage bounds or the same bounds as standard cases from which they are derived. The data for the examples and the local solutions are publicly available at [1] and can be used in testing local and global optimization techniques for OPF problems. We have observed that cases of local solutions are hard to find: indeed none was found in any of the standard test cases. However after modifying load or generator bounds local optima were found for the 9-, 39-, 118- and 300-bus cases. The examples of local optima presented in the paper are associated with either circulating flows, high line angles or an excess of reactive power. An excess of reactive power can occur when load is reduced in a network that

has been designed for peak loads. A related but less common situation that results in local optima is an excess of real power in the network. We have shown that in some cases the local OPF solutions lie within a connected feasible region, and in some cases they lie in different disconnected regions which result from the interaction of the nonlinear power flow equations with the bounds on voltage magnitudes, generator outputs or apparent power flows in lines. The SDP method of [10] worked in all except one of the standard test cases (which have no local optima), but failed in most cases in which there are local optima.

## APPENDIX

The following method was used to find paths between local optima. Let  $\mathcal{F}$  be the OPF feasible region in the space of all OPF variables, let  $S$  be an OPF solution and let  $\mathcal{H}(u_i^*)$  be a (very small) hypercube centered on  $u_i^*$ . Starting at an initial point  $u_1^*$  solve

$$u_{i+1}^* = \arg \min_{u \in \mathcal{H}(u_i^*) \cap \mathcal{F}} \|u - S\|^2$$

iteratively until a point  $u^*$  is reached where there is no further reduction in the distance from  $S$ . If at this point  $u^* = S$ , a path has been found between  $u_1^*$  and  $S$ , showing that points  $u_1^*$  and  $S$  lie in the same connected region. If however  $u^* \neq S$  a path was not found. This will always occur if  $u_1^*$  and  $S$  are in different disconnected regions, but it could also occur even if they are in the same region as a result of the path getting trapped in a local minimum of the distance to  $S$ . We chose  $u_1^*$  to be the central point of the constraints (as found by solving the OPF problem by interior point without an objective).

## REFERENCES

- [1] W. A. Bukhsh, A. Grothey, K. McKinnon, and P. A. Trodden. [Online] Available:<http://www.maths.ed.ac.uk/optenergy/LocalOpt/>.
- [2] J. Carpentier, “Contribution a l’etude du dispatching economique,” *Bull. Soc. Francaise des Electriciens*, vol. 3, pp. 431–447, 1962.
- [3] I. A. Hiskens and R. J. Davy, “Exploring the power flow solution space boundary,” *IEEE Transactions on Power Systems*, vol. 16, pp. 389–395, 2001.
- [4] J. A. Momoh, R. Koessler, M. Bond, B. Stott, D. Sun, A. Papalexopoulos, and P. Ristanovic, “Challenges to optimal power flow,” *IEEE Transactions on Power Systems*, vol. 12, pp. 444–455, 1997.
- [5] H. W. Dommel and W. F. Tinney, “Optimal power flow solutions,” *IEEE Transactions on Power Apparatus and Systems*, vol. PAS-87, pp. 1866–1876, 1968.
- [6] J. A. Momoh, R. Adapa, and M. E. El-Hawary, “A review of selected optimal power flow literature to 1993. i. nonlinear and quadratic programming approaches,” *IEEE Transactions on Power Systems*, vol. 14, pp. 96–104, 1999.
- [7] J. A. Momoh, M. E. El-Hawary, and R. Adapa, “A review of selected optimal power flow literature to 1993. ii. newton, linear programming and interior point methods,” *IEEE Transactions on Power S*, vol. 14, pp. 105–111, 1999.
- [8] Z. Qiu, G. Deconinck, and R. Belmans, “A literature survey of optimal power flow problems in the electricity market context,” in *IEEE/PES Power Systems Conference and Exposition*, 2009.
- [9] M. R. AlRashidi and M. E. El-Hawary, “Applications of computational intelligence techniques for solving the revived optimal power flow problem,” *Electric Power Systems Research*, vol. 79, pp. 694–702, 2009.
- [10] J. Lavaei and S. H. Low, “Convexification of optimal power flow problem,” in *48th Annual Allerton Conference on Communication, Control, and Computing*, 2010.
- [11] B. Zhang and D. Tse, “Geometry of injection regions of power networks,” *IEEE Transactions on Power Systems*, vol. 28, pp. 788–797, 2013.
- [12] J. Lavaei, D. Tse, and B. Zhang, “Geometry of power flows in tree networks,” in *IEEE Power and Energy Society General Meeting*, 2012.

- [13] B. C. Lesieutre, D. K. Molzahn, A. R. Borden, and C. L. DeMarco, "Examining the limits of the application of semidefinite programming to power flow problems," in *49th Annual Allerton Conference on Communication, Control, and Computing*, 2011.
- [14] A. Gopalakrishnan, A. U. Raghunathan, D. Nikovski, and L. T. Biegler, "Global optimization of optimal power flow using a branch & bound algorithm," in *50th Annual Allerton Conference on Communication, Control, and Computing*, 2012.
- [15] R. D. Zimmerman, C. E. Murillo-Sánchez, and R. J. Thomas, "Matpower: Steady-state operations, planning, and analysis tools for power systems research and education," *IEEE Transactions on Power Systems*, vol. 26, pp. 12–19, 2011.
- [16] J. Zhu, *Optimization of Power System Operation*. IEEE Press, 2009.
- [17] K. Iba, H. Suzuki, M. Egawa, and T. Watanabe, "A method for finding a pair of multiple load flow solutions in bulk power systems," *IEEE Transactions on Power Systems*, vol. 5, pp. 582–591, 1990.
- [18] A. Klos and J. Wojcicka, "Physical aspects of the nonuniqueness of load flow solutions," *International Journal of Electrical Power and Energy Systems*, vol. 13, pp. 268–276, 1991.
- [19] T. J. Overbye, "A power flow measure for unsolvable cases," *IEEE Transactions on Power Sys*, vol. 9, pp. 1359–1365, 1994.
- [20] A. J. Korsak, "On the question of uniqueness of stable load-flow solutions," *IEEE Transactions on Power Apparatus and Systems*, vol. PAS-91, pp. 1093–1100, 1972.
- [21] N. Janssens and A. Kamagaté, "Loop flows in a ring AC power system," *International Journal of Electrical Power and Energy Systems*, vol. 25, pp. 591–597, 2003.
- [22] R. D. Christie. (1999) Power systems test case archive. [Online] Available:<http://www.ee.washington.edu/research/pstca/>. University of Washington.
- [23] S. Sojoudi and J. Lavaei, "Physics of power networks makes hard optimization problems easy to solve," in *IEEE Power and Energy Society General Meeting*, 2012.
- [24] A. Wächter and L. T. Biegler, "On the implementation of an interior-point filter line-search algorithm for large-scale nonlinear programming," *Mathematical Programming*, vol. 106, pp. 25–57, 2006.
- [25] R. H. Byrd, J. Nocedal, and R. A. Waltz, *Large-Scale Nonlinear Optimization*, ser. Nonconvex Optimization and Its Applications. Springer US, 2006, vol. 83, ch. KNITRO: An Integrated Package for Nonlinear Optimization, pp. 35–59.
- [26] P. E. Gill, W. Murray, and M. A. Saunders, "SNOPT: An SQP algorithm for large-scale constrained optimization," *SIAM Journal on Optimization*, vol. 12, pp. 979–1006, 2002.